Observation of Columnar Microstructure in Step-Graded $Si_{1-x}Ge_x/Si$ Films Using High-Resolution X-Ray Microdiffraction

D. E. Eastman, C. B. Stagarescu, and G. Xu
James Franck Institute, University of Chicago, 5640 S. Ellis Avenue, Chicago, Illinois 60637

P. M. Mooney and J. L. Jordan-Sweet
IBM T. J. Watson Research Center, Yorktown Heights, New York 10598

B. Lai and Z. Cai
Experimental Facilities Division, Advanced Photon Source, Argonne National Laboratory, Argonne, Illinois 60439
(Received 8 October 2001; published 27 March 2002)

Columnar microstructure in step-graded $Si_{1-x}Ge_x/Si(001)$ structures with low threading dislocation densities has been determined using high angular resolution (~0.005°) x-ray microdiffraction. X-ray rocking curves of a 3-μm-thick strain-relaxed $Si_{0.83}Ge_{0.17}$ film show many sharp peaks and can be simulated with a model having a set of Gaussians having narrow angular widths (0.013°–0.02°) and local ranges of tilt angles varying from 0.05° to 0.2°. These peaks correspond to individual tilted rectangular columnar micrograins having similar (001) lattice spacings and average areas of 0.8 to 2.0 μm^2.

DOI: 10.1103/PhysRevLett.88.156101 PACS numbers: 68.55.–a, 61.10.Eq, 61.72.Lk

$Si_{1-x}Ge_x/Si(001)$ heterostructures are currently used for high speed bipolar transistors for communications applications [1] and have potential for high speed field effect transistors (FETs) [2,3]. Electron microscopy studies have shown that epitaxial $Si_{1-x}Ge_x$ layers with $x < 0.5$ on Si(001) relax by the introduction of 60° misfit dislocations [2,4], with misfit segments running in perpendicular ⟨110⟩ directions parallel to the wafer surface and terminating in threading arms that run up to the wafer surface. Compositionally graded $Si_{1-x}Ge_x$ buffer layers [3] have low threading dislocation densities (typically $\sim 10^5$–10^7 cm^{-2}) and are therefore useful for FETs.

Strain-relaxed epitaxial films such as $Si_{1-x}Ge_x/Si(001)$ exhibit "mosaic broadening" originating from the misfit dislocations that relieve the strain [2]. Monochromatic x-ray microdiffraction with beam footprints of 0.1–10 μm^2 have recently become available. Such measurements on step-graded relaxed $Si_{1-x}Ge_x$ films have revealed local tilted regions having the same lattice parameter ($\delta d/d \leq 5 \times 10^{-4}$) and a range of tilt angles up to ~0.25° [5]. However, the lateral dimension of the tilted regions could be only roughly estimated (<20 μm), due to the high divergence of the available x rays. Here we report x-ray microdiffraction results from the same $Si_{1-x}Ge_x$ films using a high angular resolution (~0.005°) x-ray microbeam, which provides the first detailed description of the microstructure. The microstructure of these relaxed $Si_{1-x}Ge_x$ layers is well described by a model in which the SiGe layer consists of rectangular columnar micrograins having boundaries consisting of walls of dislocations, similar to the model first proposed by Darwin to describe mosaic structure observed in bulk crystals [6].

Two $Si_{1-x}Ge_x$ structures grown at ~550 °C by ultrahigh vacuum chemical vapor deposition [7] were investigated. S1 is a Si(001) substrate with a 0.5-μm-thick $Si_{1-x}Ge_x$ layer with composition step graded from $x = 0$ to $x = 0.17$, capped with a 3-μm-thick $Si_{0.83}Ge_{0.17}$ layer having 97% of the lattice mismatch strain relaxed. S2 is a Si(001) substrate with $Si_{1-x}Ge_x$ layers as follows: 43-nm-thick $Si_{0.95}Ge_{0.05}$, 43-nm-thick $Si_{0.91}Ge_{0.09}$, 349-nm-thick $Si_{0.87}Ge_{0.13}$, and 257-nm-thick $Si_{0.83}Ge_{0.17}$. Strain relaxation in S2 is negligible (~1%) [8].

Microdiffraction experiments were performed with a high brilliance x-ray undulator source at the 2-ID-D end station [9] of the Advanced Photon Source (APS), Argonne National Laboratory. A photon energy of 8.05 keV ($\lambda = 1.54$ Å) was used and the Bragg angle (θ) was about 34° for the (004) reflection of the $Si_{1-x}Ge_x$ films and Si substrates. High angular resolution measurements were performed with an incident beam having a divergence of 0.0033° horizontal by 0.0008° vertical and a 2.7-μm diameter pinhole with a diffraction divergence of 0.004°. Microdiffraction from the Si(001) substrate gave a FWHM of the rocking curve of 0.005° for the Si(004) reflection. X-ray rocking curves were taken as a function of sample position using two detection schemes: (1) one-dimensional (1D) intensity vs θ rocking curves using a NaI scintillation detector with slits set to accept (integrate over) $\Delta(2\theta) = 0.1°$ and $\Delta\chi = 0.3°$ and (2) two-dimensional (2D) intensity maps (frames) in the 2θ-χ plane vs θ using a charge-coupled device (CCD) detector. Here 2θ is the Bragg scattering angle at the detector and χ is the vertical scattering angle perpendicular to the horizontal diffraction plane. The CCD detector has 1241 (horizontal) × 1152 (vertical) square pixels, 54.6 μm on a side, which corresponds to an effective resolution per pixel of ~0.003° in 2θ and χ. Since the extinction depth at the Bragg peak (~3–8 μm at $\lambda = 1.54$ Å for Si) is greater than the

SiGe film thickness, the full lateral areas illuminated by the beam become $\sim 22\ \mu m^2$ for sample S1 and $\sim 12\ \mu m^2$ for sample S2.

Figure 1 shows 1D rocking curves for S1. Figure 1(a) depicts an overview of the rocking curves taken at 50 different vertical y positions that display a complex variety of shapes and wide range of tilt angles. The θ spread varies locally from $\sim 0.03°$ [Fig. 1(b)] to $\sim 0.2°$ [Fig. 1(c)]. All spectra show a complex fine structure on a scale of $\sim 0.01°$–$0.02°$. This fine structure is resolved for the first time.

We have directly measured the microdiffraction χ and 2θ scattering angles of the individual "micrograins" using a 2D CCD detector. Sets of two-dimensional scattering intensity maps or picture frames (in the 2θ-χ plane) were taken at each θ value (0.002° steps were used). Figure 2 shows three of the many 2θ-χ frames and a plot of the integrated intensity of each frame vs θ, namely, the rocking curve. The Si(004) Bragg angle θ_B is $\sim 34°$, and measured vertical CCD angle χ_{CCD} and width $\Delta\chi_{CCD}$ are larger than the actual tilt angle χ_{sample} and width $\Delta\chi_{sample}$ by the kinematic factor $2\sin\theta_B = 1.1$ [10]. The frame on the right in Fig. 2 shows diffraction spots from the largest micrograin and the smaller one just to its right, both having FWHM widths of $\Delta(2\theta) \cong 0.01°$ and $\Delta\chi \cong 0.01°$. In the middle picture, two micrograins separated by $\Delta\chi \cong 0.05°$ are seen plus a small micrograin between them, as well as some diffuse scattering background; this indicates that 1D rocking curves integrate over such redundancies. The picture on the left shows an unusual case where five discrete micrograins are seen in a $\Delta\chi$ range of $\sim 0.1°$ and a $\Delta(2\theta)$ range of $\sim 0.045°$, an unusually large spread in $\Delta(2\theta)$. A significant diffuse background ($\sim 20\%$–30%) is also seen in this frame. We find that nearly all the scattering intensity consists of narrow peaks from tilted micrograins with a well-defined $\Delta(2\theta) \leq 0.02°$ and $\Delta\chi \leq 0.015°$. These 2D pictures allow us to estimate the degree of degeneracy, i.e., unobserved micrograins, in 1D rocking curves taken with the NaI detector. When relatively intense peaks (large micrograins) are present such as in the right frame, we generally saw little redundancy. When small micrograins are present, e.g., in the left and center frames, a redundancy of ~ 1.5 to 3 is estimated for resolved peaks in 1D rocking curves. Also, we cannot resolve micrograins with tilt angle differences less than our angular resolution (0.005°).

Additional insight is gained by studying S2, which has a very low misfit dislocation density and two detectable

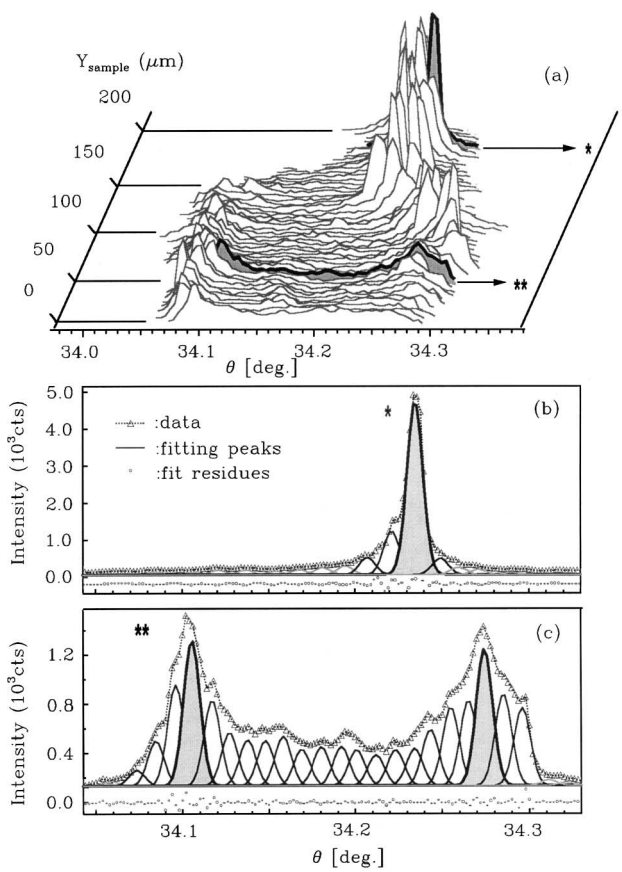

FIG. 1. (a) Series of rocking curves for sample S1 taken in 4.0-μm vertical position steps ("θ-y" map). (b) Example of a narrow rocking curve dominated by a single sharp peak. This peak contains $\sim 56\%$ of the total area. (c) Example of a broad, two-lobed rocking curve with a θ range of $\sim 0.2°$. The two highlighted Gaussians have an area of $\sim 10\%$ of the total area.

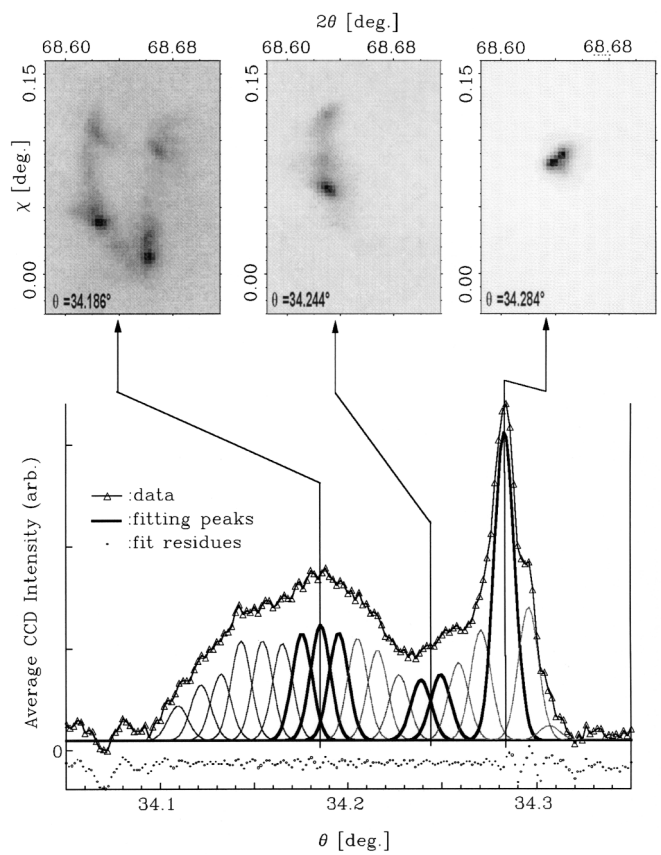

FIG. 2. Integrated CCD rocking curve from sample S1 with a 0.002° θ step. The three 2D pictures at the top show scattering intensity distributions in the 2θ-χ plane.

$Si_{1-x}Ge_x$ layers. Figure 3(a) shows rocking curves for S2 at three different y positions. Because of their different alloy compositions, the two layers have measurably different lattice parameters, $\Delta\theta_B^{L2-L1} \cong 0.108°$. Thus their rocking curves can be recorded separately by repositioning the detector arm by $\Delta(2\theta)_B^{L2-L1} \cong 0.216°$ and using a slit having an acceptance angle of $\Delta(2\theta)_{\text{acceptance}}^{\text{NaI}} \cong 0.1°$. We have overlaid the rocking curves of the lower layer L2 ($Si_{0.87}Ge_{0.13}$) and the upper layer L1 ($Si_{0.83}Ge_{0.17}$) by shifting the former by the difference in macroscopic average Bragg angles of ~0.108°. The rocking curves for the two layers show a strong resemblance in spectral shape. Another measurement of these two layers that depicts the similarity of their diffraction is shown in Fig. 3(b), where the diffraction intensity at constant angle of incidence is plotted versus horizontal sample position (2-μm steps). The intensity variation in the two scans is strikingly similar, indicating that the perturbation of the crystal lattice by the misfit dislocations at the SiGe/Si interface extends throughout the entire SiGe film. This result is consistent with a recent experiment showing that the strain field of a buried dislocation perturbs the surface of the sample [11]. These measurements suggest that the tilted micrograins observed in S1 are "columnar" in nature, extending from the misfit dislocation network underneath the $Si_{1-x}Ge_x$ layers through their entire thickness.

Step-graded $Si_{1-x}Ge_x$/Si(001) structures grown under our conditions are known to relax by a dislocation multiplication mechanism in which pileups of 60° misfit dislocations extending below the $Si_{1-x}Ge_x$/Si interface are formed [3,5]. Since the misfit segments lie in the two perpendicular ⟨110⟩ directions parallel to the wafer surface, the tilted columnar micrograins that result from the dislocation pileups have rectangular cross sections in the plane

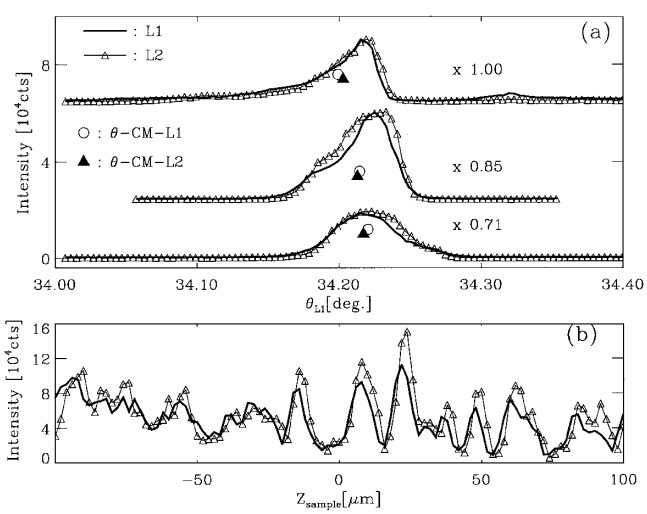

FIG. 3. (a) Rocking curves from both layers of sample S2. The θ "centers-of-mass" positions are shown. (b) Diffraction intensity at constant angle θ_1 and θ_2 of incidence; $\theta_1 = 34.073°$ for film L1 and $\theta_2 = 33.964°$ for film L2 versus horizontal sample position z (2-μm steps).

of the wafer and low angle grain boundaries underneath that are {111} lattice planes. We have estimated the ranges of tilt angles and sizes of the tilted micrograins for sample S1 using a simple model in which each micrograin is described by a Gaussian peak with a tilt angle and fixed angular width. The optimum Gaussian FWHM was found to be 0.013° from fitting peaks as shown in Figs. 1(b) and 1(c) and individual tilt angles and intensities (Gaussian amplitudes) were determined by fitting the 1D rocking curves. In this columnar microstructure model, the diffracted intensity from a micrograin is proportional to its illuminated volume, which we approximate as an effective rectangular cross-sectional area extending through the film thickness. The sum of all illuminated micrograins is taken to be proportional to the total integrated intensity of the rocking curve. Experimentally, we have found for θ vs y sets of rocking curves that the integrated total intensities of many curves are constant to within ±5%–6% (typically) or ≤±18% (worst case). We have calculated the illuminated areas from the beam dimensions, angle of incidence (θ), and film thickness. Knife-edge measurements were used to determine the horizontal and vertical dimensions of the beam and gave 3.0 × 2.5-μm FWHM, with an area at normal incidence of ~6 μm^2.

The fitting procedure uses an iterative fitting algorithm [12] and starts with a set of initial guesses and a low number of Gaussians, typically 5 to 15 Gaussians quasi-equidistantly spaced in θ. The fitting procedure is allowed to freely change the Gaussian peaks' positions and amplitudes while holding their FWHM constant: thus, they correspond in our model to grains of various sizes and tilting angles but otherwise are made of identical material (same "intrinsic" diffraction width). The number of Gaussians is then increased until there is no further improvement in χ^2. This corresponds to the minimal Gaussian set required to describe a given rocking curve. The sizes of the Gaussians fitted to 1D detector rocking curves were corrected for angle redundancies using a qualitative analysis of all the frames of a number of 2D CCD rocking curves. We estimate that a moderate redundancy (~1.0 to 1.5) of micrograins in 1D NaI detector θ scans occurs for narrow (≤0.05°) and medium (~0.05°–0.12°) width rocking curves from large micrograins (~1.0–9.0 μm^2), while a large redundancy (~2.0 to 3.0) occurs in wide (~0.2°) rocking curves from the smaller micrograins such as Fig. 1(c). In the latter case, the local tilt angles and intensities of the fitted Gaussians have more uncertainty ($\Delta\theta_T \approx 0.013°$).

We have fitted ≥100 NaI scintillation detector rocking curves taken at many different sample positions (typically 5-μm steps) representing a total sampled area of ~10^4 μm^2 for sample S1 and have studied the distributions of sizes and tilt angles of the columnar micrograins. θ vs y rocking curves were taken stepping along both ⟨100⟩ and ⟨110⟩ directions and similar ranges of tilt angles were observed. Using our Gaussian fitting model and

the above redundancy correction factors, we have the following general description of the microstructure for sample S1. Rectangular micrograins that have tilted lattice planes, characterized by individual rocking curves having a FWHM of $\sim 0.013°-0.02°$ and Bragg angles that vary by $\leq 0.02°$, account for typically 80%–90% of the total scattering intensity with the remaining fraction being diffuse scattering in a range of $\leq 0.06°$ FWHM in both 2θ and χ. The most prevalent rocking curves ($\sim$50% of a total of 250) had a medium range of tilt angles ($\sim 0.05°-0.12°$) and average micrograin area of $\sim 2\ \mu m^2$ [13]. About 15% of the rocking curves had a narrow range of tilt angles ($\leq 0.05°$) with an average area of $5\ \mu m^2$ and a maximum observed area of $14\ \mu m^2$. About 35% of the rocking curves had a wide range of tilt angles ($\sim 0.12°-0.23°$), an average grain area of $0.8\ \mu m^2$, and a significant number of micrograins below $0.4\ \mu m^2$. Consistent with previous x-ray microdiffraction measurements of the same samples [5], the shapes of the rocking curves and average tilt angles tend to correlate over distances of $10-20\ \mu m$ with intermittent rapid changes in shapes and average angle.

A summary of the $Si_{1-x}Ge_x$ layer microstructure, which underlies a fundamental understanding of physical properties, is as follows. Defining widths as the square root of areas, rectangular columnar micrograins are found with average widths from ~ 0.6 to $\sim 3.7\ \mu m$, and with the vast majority between 0.8 and $1.4\ \mu m$, are found that extend from the misfit dislocation network near the SiGe/Si interface up to the wafer surface. The micrograins have similar lattice parameters ($\delta d/d \approx 5 \times 10^{-4}$), but their [001] axes are tilted up to $\sim 0.1°$ with respect to the [001] axes of the Si substrate. We also find that about 10%–20% of the diffracted intensity is diffuse scattering [$\delta(2\theta) < 0.06°$, from 2D images], which may arise from nonuniform strained material near the boundary regions between the micrograins. Cross-sectional transmission electron micrographs (e.g., Figs. 12, 16, and 33 of Ref. [2]) show that the average spacing between dislocation pileups in similar relaxed step-graded $Si_{1-x}Ge_x$ structures is $\sim 1\ \mu m$. This strongly suggests that the dislocation pileups form low angle {111} grain boundaries at the base of the columnar micrograins in step-graded $Si_{1-x}Ge_x$/Si(001). Each 60° misfit dislocation results in an atomic step on the wafer surface. When significant strain relaxation occurs, the surface morphology is characterized by a crosshatch pattern with an average lateral dimension that corresponds to the average spacing of the dislocation pileups, $\sim 1\ \mu m$ [14]. From near-field scanning optical microscopy measurements, electrical activity associated with the crosshatch surface morphology was attributed to variations in band structure due to the strain fields of misfit dislocations [15]. Our results suggest such strain variations are less than $\sim 5 \times 10^{-4}$.

The samples were grown by J. O. Chu. The APS facility is supported by the U.S. Department of Energy, Office of Science, Office of Basic Energy Sciences, under Contract No. W-31-109-ENG-38. The University of Chicago team (C. B. S., G. X., and D. E. E.) was supported in part by the DOE under Contract No. W-31-109-ENG-38.

[1] B. S. Meyerson, IBM J. Res. Dev. **44**, 391 (2000).
[2] P. M. Mooney, Mater. Sci. Eng. **17**, 105 (1996), and references therein.
[3] S. J. Koester, R. Hammond, J. O. Chu, P. M. Mooney, J. A. Ott, L. Perraud, K. A. Jenkins, S. Webster, I. Lagnado, and P. R. de la Houssaye, IEEE Electron Device Lett. **22**, 92 (2001).
[4] F. K. LeGoues, B. S. Meyerson, and J. F. Morar, Phys. Rev. Lett. **66**, 2903 (1991).
[5] P. M. Mooney, J. L. Jordan-Sweet, I. C. Noyan, S. K. Kaldor, and P.-C. Wang, Appl. Phys. Lett. **74**, 726 (1999); Physica (Amsterdam) **273B–274B**, 608 (1999).
[6] P. B. Hirsch, in *Progress in Metal Physics,* edited by B. Chalmers and R. King (Pergamon, New York, 1956), Vol. 6, pp. 236–339.
[7] B. S. Meyerson, Appl. Phys. Lett. **48**, 797 (1986).
[8] The layer thicknesses were measured by cross-sectional transmission electron microscopy. Standard x-ray diffraction measurements were used to measure the alloy composition, the degree of relaxation, and mosaic broadening. The 004 rocking curve peak from the 97% relaxed $Si_{0.83}Ge_{0.17}$ layer of S1 has a FWHM of 0.169°, much broader than the peaks from the much thinner strained $Si_{0.87}Ge_{0.13}$ and $Si_{0.83}Ge_{0.17}$ layers of S2 that have a FWHM of 0.035°.
[9] Z. Cai *et al.,* in *The Sixth International Conference for X-Ray Microscopy,* edited by W. Meyer-Ilse, T. Warwick, and D. Attwood (Springer-Verlag, Berkeley, CA, 2000), Vol. 507, p. 472.
[10] The measured vertical CCD angle χ_{CCD} is related to the sample vertical tilt angle χ_{sample} by $\chi_{CCD} = 2\sin(\theta_B)\chi_{sample}$.
[11] P. Sutter and M. G. Lagally, Phys. Rev. Lett. **82**, 1490 (1999).
[12] The nonlinear, least-squares fitting was done using the Levenberg-Marquardt algorithm to search for the coefficient values that minimize χ^2.
[13] Our columnar model underestimates micrograin areas for sample S1 since some are always partially illuminated and overestimates areas since their actual heights are less than the 3-μm film thickness due to {111} grain boundaries. Both these effects are estimated to be $\sim$20%–40% corrections and tend to cancel each other.
[14] M. A. Lutz, R. M. Feenstra, F. K. LeGoues, P. M. Mooney, and J. O. Chu, Appl. Phys. Lett. **66**, 724 (1995).
[15] M. H. Gray, J. W. P. Hsu, L. Giovane, and M. T. Bulsara, Phys. Rev. Lett. **86**, 3598 (2001).